CrystEngComm

PAPER

View Article Online
View Journal | View Issue

Cite this: *CrystEngComm*, 2014, **16**, 3730

Simple dinitro substituted calix[4]arene forming a honeycomb-like architecture with hydrophobic channels†

Tobias Gruber,*[a] Frank Eißmann,[a] Margit Gruner,[b] Luisa G. Heinz,‡[a] Wilhelm Seichter[a] and Edwin Weber*[a]

Received 9th September 2013,
Accepted 31st October 2013

DOI: 10.1039/c3ce41819g

www.rsc.org/crystengcomm

A rather easily structured permethylated dinitro calix[4]arene was found to exhibit large, stable and rigid channels in the solid state. These were obtained as guest free as well as solvent filled species and proved to reversibly adsorb selected organic solvents. Combined use of QMB measurements and X-ray powder diffraction revealed the predominantly reversible interaction of dichloromethane vapour with the channel structure as well as the integrity of the nanopores during adsorption and desorption. Examination of the flexible host component by NMR spectroscopy revealed a mixture of interchanging conformational isomers which could explain the high sensitivity of the crystallization process from the employed solvents.

Introduction

Microporous solids[1] are still of unbroken interest in supramolecular chemistry[2] since they show outstanding properties, *e.g.* as catalysts or for purposes of gas storage[3] and nonlinear optics.[4] Currently, the well-examined zeolites[5] of purely inorganic nature undergo extension by the use of organic constituents, leading to the concept of metal–organic frameworks (MOFs)[6] that are rapidly developing due to their promising applications.[7] A third emerging class of porous materials is generated *via* self-assembly of purely organic compounds to yield the so-called 'organic zeolites'.[8] Hence, the creation of stable, non-penetrated or guest-independent non-collapsing porous materials is a highly topical challenge. In order to satisfy the requirements of such a porous material, the molecular components assembling the aggregate structure are expected to behave as rigid tectonic building units.[9] In a few examples, derivatives of calixarenes that correspond to this concept have actually been described to yield a nanoporous supramolecular structure.[10]

Here, we report on a special case of a porous material featuring hydrophobic channels formed by a conformationally flexible calix[4]arene (Scheme 1). Most remarkably, the channels can be obtained as guest free and solvent filled species, or the channels are not formed at all depending on the solvent of crystallization. The title compound is a rather basic calixarene, and despite its presence in the literature for over a decade,[11] until today, no X-ray structure of this compound has been described.

Results and discussion

The crystal structures of the solvent-free calixarene **1** and of its inclusion compound with acetone (**1a**) have the rhombohedral space group $R\bar{3}$ with nearly identical cell parameters (Table 1). According to the three-fold crystal symmetry, the smallest supramolecular entities of the crystal structures are represented by cyclic hexamers of calixarene molecules (Fig. 1a) which are further arranged in a columnar fashion along the crystallographic *c*-axis, thus creating channel-like voids with a diameter of approximately 6 Å. The total solvent accessible void volumes per unit cell are 1675 Å^3 for **1** and 1612 Å^3 for **1a**, which correspond to 12.0 and 11.6% of the respective cell volumes. Due to the absence of strong hydrogen bond donors, each of the hexamers is stabilized by a close network of C–H···O hydrogen bonds[12] [d(H···O) = 2.60–2.72 Å] in which the nitro groups as well as methylene and arene hydrogens take part (Table S1, ESI†).

When a chloroform–toluene mixture was used for crystallization, the crystal structure turned out to be the guest-free species, *viz.* the cavity spanned by six calixarene molecules is empty. On the other hand, crystallization from acetone–toluene

[a] *TU Bergakademie Freiberg, Institut für Organische Chemie, Leipziger Str. 29, 09596 Freiberg, Sachsen, Germany. E-mail: tobias.gruber@chemie-tu-freiberg.de, edwin.weber@chemie.tu-freiberg.de*
[b] *TU Dresden, Institut für Organische Chemie, Mommsenstr. 13, 01062 Dresden, Germany*

† Electronic supplementary information (ESI) available: Representations of the acetone disorder and packing structure of **1a** (Fig. S1), crucial hydrogen bonds in the X-ray structure of **1**–**1b**, as well as 1D and 2D NMR data of **1** in $CDCl_3$ (Fig. S2–S11, Tables S2–S4). CCDC 787340, 787341 and 870204. For ESI and crystallographic data in CIF or other electronic format see DOI: 10.1039/c3ce41819g

‡ Present address: Universität Basel, Institut für Anorganische Chemie, St. Johanns-Ring 19, 4056 Basel, Switzerland.

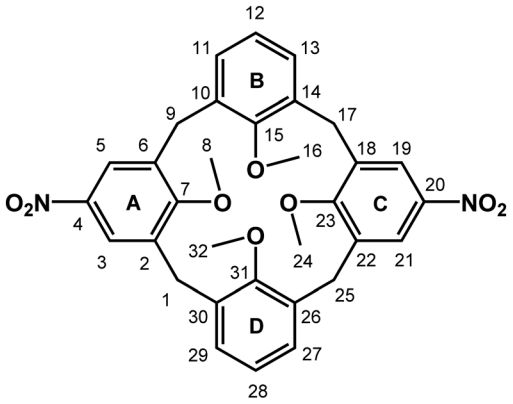

1

1a: **1**· acetone (3 : 1)
1b: **1**· $CHCl_3$ (1 : 1)

Scheme 1 Compounds studied in this paper.

yielded an isostructural 3 : 1 exo-complex with acetone (**1a**), which shows the acetone molecule disordered around a three-fold rotational inversion axis within this very cavity (Fig. S1, ESI†). The partially solvated structure can be explained by an incomplete evaporation of the acetone during or after formation of the crystals and is probably associated with its perfect match and slightly better host–guest van der Waals interactions in comparison to chloroform or toluene.

On closer examination, we found that, in both structures of **1**, the calixarenes deviate significantly from the characteristic cup-shape and develop extremely pinched cone conformations (C_{2v} symmetry, Fig. 1b). In general, the adoption of a cone conformation for the flexible tetramethoxy calix[4]arenes in the solid state is, with the exception of the respective sodium complex,[13] a rather atypical behaviour as previously shown by our and other groups.[14] However so far, only phenyl substituted and some laterally derivatized tetramethoxy calixarenes were found to be in the cone conformation in the crystal.[15] Furthermore, in the present structures of title compound **1**, the cone conformation is rather impaired and could probably be best described as inverted: the arene units A and C are almost coplanar (interplanar angles of 16.7° and 16.0°, respectively) with the nitro groups pointing at each other, forcing the aromatic rings B and D to open widely (apex angles of 115.1° and 114.7°, respectively) (Table 2). This striking arrangement of the aromatic building units is accompanied by a narrowing of the intramolecular cavity, preventing cavity formation with the respective solvent molecules, and can be explained on the one hand by the absence of coordinating substituents at the lower rim and on the other hand by strong steric demands of the crystal packing.

Table 1 Crystal data and selected details of the data collection and refinement calculations of compounds **1**, **1a** and **1b**

Compound	**1**	**1a**	**1b**
Empirical formula	$C_{32}H_{30}N_2O_8$	$C_{32}H_{30}N_2O_8\cdots0.33\ C_3H_6O$	$C_{32}H_{30}N_2O_8\cdots CHCl_3$
Formula weight	570.58	589.94	689.95
Crystal system	Rhombohedral	Rhombohedral	Orthorhombic
Space group	$R\bar{3}$	$R\bar{3}$	*Pbca*
a/Å	39.4134(4)	39.3244(3)	16.1514(5)
b/Å	39.4134(4)	39.3244(3)	16.4165(5)
c/Å	10.4024(2)	10.4186(2)	24.4814(8)
α/°	90.0	90.0	90.0
β/°	90.0	90.0	90.0
γ/°	120.0	120.0	90.0
V/Å^3	13 994.3(3)	13 952.9(3)	6491.2(4)
Z	18	18	8
F(000)	5400	5592	2864
D_c/g cm^{-3}	1.219	1.264	1.412
μ/mm^{-1}	0.088	0.092	0.337
Data collection:			
Temperature/K	93(2)	103(2)	100(2)
No. of collected reflections	114 418	105 784	45 746
Within the θ-limit/°	2.1–29.1	2.1–28.6	1.7–26.1
Index ranges $\pm h$, $\pm k$, $\pm l$	−53/53, −53/52, −14/11	−45/52, −51/52, −13/14	−19/19, −20/20, −30/29
No. of unique reflections	8290	7896	6445
R_{int}	0.0477	0.0566	0.0369
Refinement calculations: full-matrix least-squares on all F^2 values			
Weighting expression w^a	$[\sigma^2(F_o^2) + (0.0877P)^2 + 17.1128P]^{-1}$	$[\sigma^2(F_o^2) + (0.0600P)^2 + 22.8232P]^{-1}$	$[\sigma^2(F_o^2) + (0.0957P)^2 + 9.2233P]^{-1}$
No. of refined parameters	383	399	444
No. of F values used $[I > 2\sigma(I)]$	6448	5211	5278
Final R-indices			
$R = (\sum\|\Delta F\|/\sum\|F_o\|)$	0.0496	0.0531	0.0678
wR on F^2	0.1494	0.1462	0.2150
S = (goodness of fit on F^2)	0.995	1.041	1.284
Final $\Delta\rho_{max}/\Delta\rho_{min}$/e Å^{-3}	0.55/−0.36	0.44/−0.29	0.88/−0.53

[a] $P = (F_o^2 + 2F_c^2)/3$.

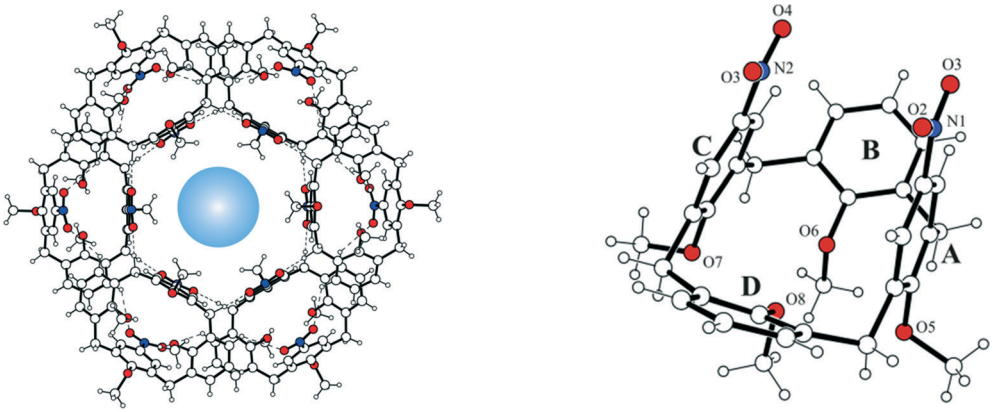

Fig. 1 a) Structure of the hexameric calixarene unit of **1a** viewed down the crystallographic *c*-axis. Broken lines represent hydrogen bonds. Because of the high grade of disorder, the acetone molecule in the channels has been omitted for clarity and is marked by a light blue circle. A detailed representation of the acetone disorder is shown in Fig. S1, ESI.† b) Molecular structure of **1**.

Table 2 Selected conformational parameters of the compounds studied in this paper

Compound	1	1a	1b
Interplanar angles (°)[a]			
A/C	16.7(1)	16.0(1)	24.9(1)
B/D	64.9(1)	65.3(1)	70.6(1)
mpla[b] /A	84.7(1)	85.2(1)	78.0(1)
mpla/B	30.4(1)	34.6(1)	24.6(1)
mpla/C	78.6(1)	78.9(1)	77.1(1)
mpla/D	34.5(1)	30.7(1)	85.0(1)
Ring A/NO_2 group	3.5(2)	2.8(1)	22.1(1)
Ring C/NO_2 group	6.4(2)	6.6(2)	13.4(1)

[a] Aromatic rings: ring A: C(2)…C(7); ring B: C(10)…C(15); ring C: C(18)…C(23); ring D: C(26)…C(31). [b] Best plane through atoms C(1), C(9), C(17) and C(25).

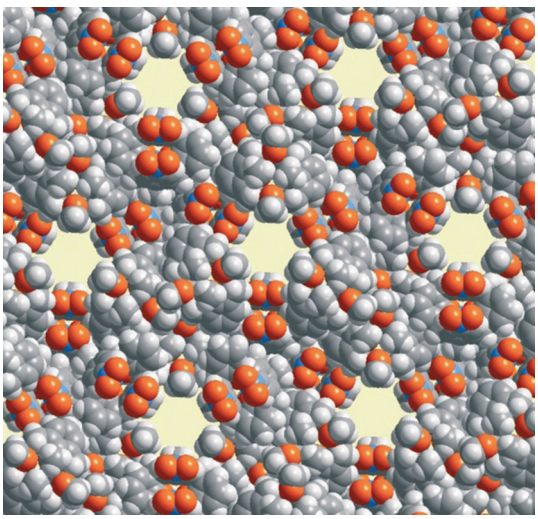

Fig. 2 Structure of the crystal lattice of **1** viewed down the crystallographic *c*-axis. Carbon atoms are displayed as grey spheres, and oxygens as red spheres.

As depicted in Fig. 2, the overall packing structure is characterized by a columnar arrangement of calixarene hexamers along the crystallographic *c*-axis. Because of the relatively low polar nature of the hexamers, the crystal structure is predominantly stabilized by van der Waals type forces and weak intermolecular packing interactions. The surface of the hexameric unit, as well as the interior of its cavity, is formed by methoxy groups.

Surprisingly, slight changes in the solvent system used for the crystallization of the title compound result in a completely different crystal structure. When we used chloroform–*n*-hexane instead of chloroform–toluene, a 1 : 1 inclusion compound of **1** with $CHCl_3$ (**1b**) in the orthorhombic space group *Pbca* was recovered. Remarkably, the calixarene adopts in this case a partial cone conformation (Fig. 3) with interplanar angles of 70.6(1)° for rings B/D and 24.9(1)° for rings A/C. Like in the above cone form, the very narrow cavity prohibits the formation of an *endo* complex with solvent molecules. And yet, in the present case, chloroform is clathrate-like accommodated in the lattice voids. The guest molecule shows a twofold disorder with SOFs of 0.858 (C1G, Cl1G, Cl2G, Cl3G, H1G) and 0.142 (C1H, Cl1H, Cl2S, Cl3H, H1H), respectively. Interestingly, within the packing of the sheet-like arranged calixarene molecules, the two differently occupied positions of the chloroform display distinct intermolecular interactions. For disorder position 1 (Fig. 4a), the $CHCl_3$ guest is only engaged in one bifurcated C–H···O hydrogen bond,[16] though in the minor occupied chloroform position 2, additional strong C–H···Cl hydrogen bonds[17] [*d*(H···Cl) 1.84 Å] and weak head-on Cl···Cl contacts[16] [*d*(Cl···Cl) 2.902(5) Å] can be observed (Fig. 4b). The interconnection of the calixarene molecules among themselves is restricted to two weak C–H···O-contacts involving two of the methylene bridges and two oxygen atoms of the nitro groups.

The above findings stimulated a thorough conformational analysis of the title molecule in solution. A complex pattern of signals in the NMR spectra in $CDCl_3$ and $CDCl_3$–toluene-d_8 indicates the existence of different conformers. Detailed 2D

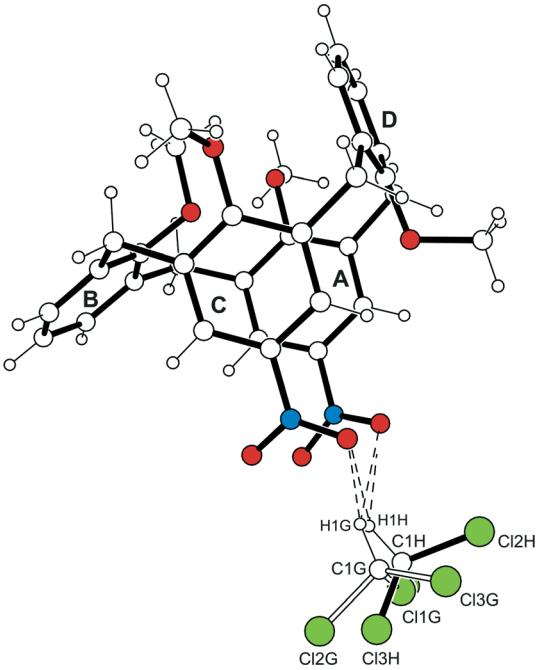

Fig. 3 Molecular structure of the 1:1 complex of **1** with $CHCl_3$ (**1b**). Broken lines represent hydrogen bonds. The two disorder sites of the guest molecule are marked by different styles of bonds.

NMR studies using COSY, $^{1}H/^{13}C$ correlated HSQC and HMBC, as well as subsequently applied NOESY and ROESY methods lead to a full assignment of the conformative structures (Fig. S2–S11, Tables S2–S4, ESI†) and their distribution in solution, as summarized in Fig. 5 and Table 3.

In general, only one cone conformation and two partial cone conformations are observed in this system, though potential alternate conformations are not detected in any case. For **1** in chloroform–toluene (from which the respective guest free channel structure was obtained), all three forms occur in a 1:2:2 ratio at room temperature with 21% cone, 39% partial cone 1 and 40% partial cone 2. By using $CDCl_3$–*n*-hexane-d_{14} or pure chloroform, the ratios of the different conformers do not change significantly. In all cases, the somewhat non-polar partial cone species are favoured, which leads also to the manifestation of one of these conformations in the solid state in the case of crystallization from chloroform–*n*-hexane. However, crystal formation of **1** in chloroform–toluene prefers the cone form of the title molecule. It seems feasible that the chloroform evaporates more easily, leaving behind a solution of **1** that is rich in toluene. In that case, the formation of 1:1 inclusion complexes of the title compound with toluene can be discussed, accompanied by a conformational swing towards the cone form, which is also present in the inclusion compounds **1a** and **1b**. The subtle influence of solvents and respective mixtures on the solid state behaviour of a calixarene was only recently discussed in the literature.[18]

For a general estimation of the conformational changes caused by the nitration of the parent tetramethoxy calix[4]arene, it seemed reasonable to include the conformer distribution of the respective unsubstituted[19] and tetranitro[20] calix[4]arenes

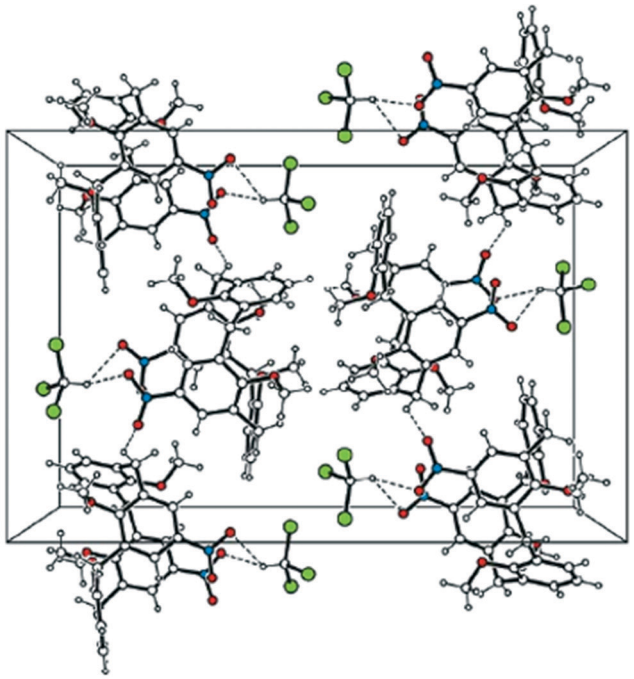

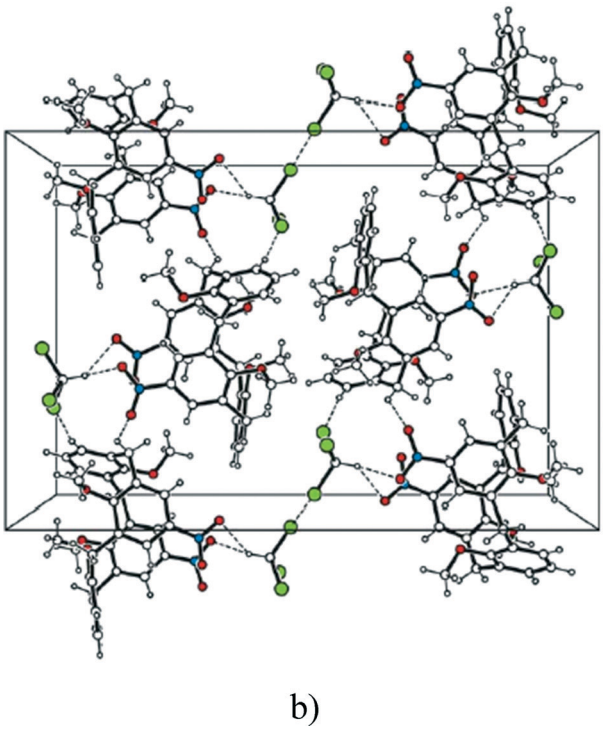

Fig. 4 Packing structure of the 1:1 complex of **1** with $CHCl_3$ (**1b**) viewed down the crystallographic *a*-axis with the respective major-occupancy component (a) and minor-occupancy component of the solvent molecule (b). Broken lines indicate intermolecular interactions.

(22% cone/78% partial cone and 7% cone/93% partial cone, respectively, *vs.* 21% cone/79% partial cone for **1**). Hence, the conformational behaviour of the tetramethoxycalix[4]arene in $CDCl_3$ varies only little by introduction of two nitro groups

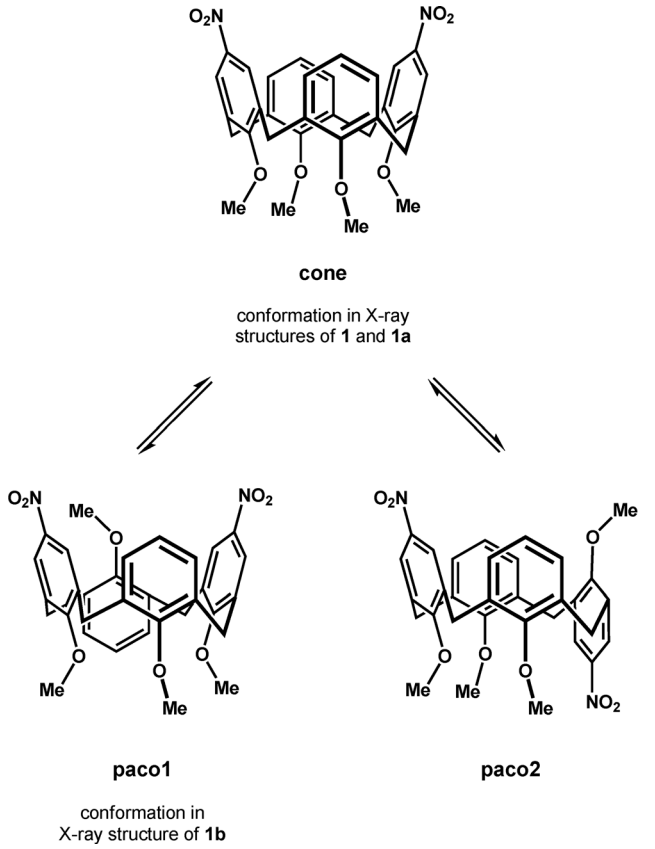

Fig. 5 Conformational transformations of **1** in solution.

Table 3 Distribution of the conformers of **1** in solutions of $CDCl_3$, $CDCl_3$–toluene-d_8 or $CDCl_3$–*n*-hexane-d_{14} at different temperatures (mol%). Alternate conformations were not observed. Please note that it was not possible to determine the conformational distribution of **1** in pure toluene-d_8 as the compound is only sparingly soluble in this solvent

Conformer	Cone	Partial cone 1	Partial cone 2
$CDCl_3$–toluene-d_8, T = 295 K	21	39	40
$CDCl_3$–toluene-d_8, T = 262 K	20	48	32
$CDCl_3$ T = 295 K	20	43	37
$CDCl_3$ T = 262 K	19	48	33
$CDCl_3$–*n*-hexane-d_{14}, T = 295 K	23	43	34
$CDCl_3$–*n*-hexane-d_{14}, T = 262 K	21	43	36

at the upper rim. However, exhaustive nitration of the upper rim increases the rate of partial cone conformation up to 93%.

In a next step, a quartz microbalance device[21] was used to determine the sorptive property of apo-host **1** towards varying solvent vapours that are exemplary of high and low polarity as well as of protic and aprotic nature (*n*-hexane, dichloromethane, tetrahydrofuran, acetone, ethanol, toluene, cyclohexene and cyclohexane). The results obtained are as follows (Fig. 6): the vapours of the more or less polar aprotic solvents

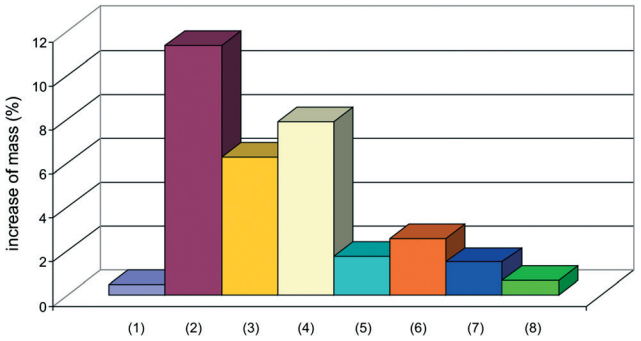

Fig. 6 Responses of a QMB device coated with **1** for vapours of various solvents: (1) *n*-hexane, (2) dichloromethane, (3) tetrahydrofuran, (4) acetone, (5) ethanol, (6) toluene, (7) cyclohexene, and (8) cyclohexane.

dichloromethane, acetone and tetrahydrofuran are adsorbed rather intensively, while the adsorption of the polar protic (ethanol) and non-polar solvents (*n*-hexane, cyclohexene, cyclohexane, and toluene) is not significant. All this behaviour is likely to be connected with the polarity interrelation between the adsorbed compound and the solid adsorbent.

As demonstrated by previous studies,[22] depending on the size and interaction of the analyte molecules, the regeneration step of a quartz microbalance does not always return the sensor frequency to the starting value, which is undoubtedly necessary for a possible application of this nanoporous material for the sensing or storage of organic vapours. As shown in Fig. 7 for dichloromethane as an example, the rate of regeneration, *viz.* the return of the frequency of the oscillating quartz to the original level, for this special case is larger than 99.99%. Hence, the pores display a rather low host affinity, which is a consequence of missing interaction between host and guest, but nevertheless enable fast and reversible guest diffusion.

Despite the weak intermolecular interactions within the solid, the macroscopic crystals of guest-free **1** turned out to

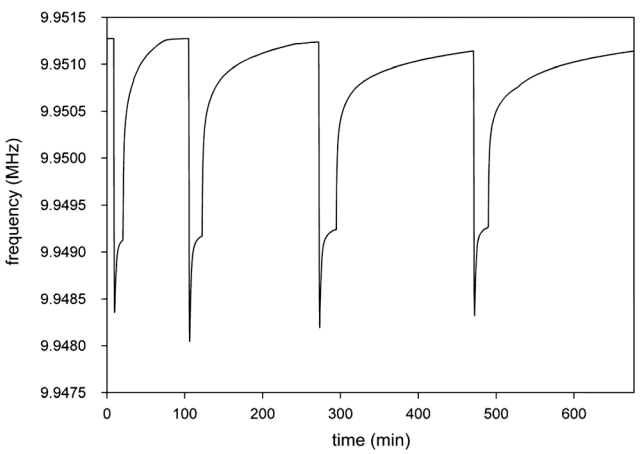

Fig. 7 QMB dichloromethane vapour sorption measurements of a coating of **1** showing four adsorption–desorption cycles. Solvent adsorption leads to a spontaneous decrease in frequency and finally a frequency equilibration. Desorption and the related adjustment to equilibrium frequency occur more slowly.

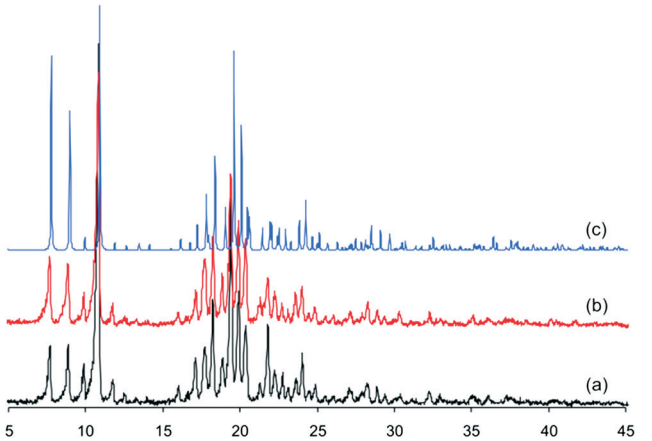

Fig. 8 X-ray powder pattern of **1** before adsorption (a) and after desorption (b) of dichloromethane. For comparison, (c) shows the pattern calculated from the single crystal analysis of the guest-free structure of the title compound.

be perfectly air-stable. To demonstrate the preservation of the nanopores even after adsorption and desorption of organic guests, powder diffraction was used (Fig. 8). Comparison of the X-ray powder diffraction patterns of **1** before adsorption and after desorption of dichloromethane reveals no significant differences and suggests the integrity of the nanopores even in the presence of solvent vapour.

Conclusion

In summary, we have identified a total organic framework featuring large, stable and rigid channels composed of hexameric units of a dinitro tetramethoxy calixarene. Examination by NMR spectroscopy revealed a high sensitivity of the crystallization process from the employed solvents. In order to elucidate the adsorption properties of the nanoporous material on hand, we combined the use of QMB measurements and X-ray powder diffraction. Examining selected organic solvent vapours, dichloromethane turned out to be the most promising candidate for further inclusion experiments, which revealed the predominantly reversible interaction of the dichloromethane vapour with the channel structure as well as the integrity of the nanopores during adsorption and desorption. In subsequent studies, we will elucidate to what extent the title calixarene can be derivatised without losing the ability to form a nanoporous material in the solid state.

Experimental section

Materials

The title calixarene **1** was obtained straightforwardly by nitration of the corresponding dimethoxy calix[4]arene[23] followed by exhaustive methylation using methyl iodide and potassium carbonate.[11] Thereupon, compound **1** was dissolved in a mixture of chloroform–toluene (1 : 1) or acetone–toluene (1 : 1), respectively, which afforded diffraction quality single crystals of **1** and **1a** (in both cases; the solvents were allowed to evaporate completely). When we used chloroform–*n*-hexane instead of chloroform–toluene, a 1 : 1 inclusion compound of **1** with $CHCl_3$ (**1b**) was recovered.

X-ray crystal structure analysis

Diffraction data were collected using a Bruker Kappa APEX II CCD diffractometer with MoK_α radiation (λ = 0.71073 Å). Intensities were corrected for absorption using the multi-scan technique *SADABS*.[24] Structure solution and refinement were carried out using *SHELXS-97* and *SHELXL-97*.[25] All non-hydrogen atoms were refined anisotropically (except for the case of the disordered acetone in **1a**); H atoms were fixed in calculated positions, and the H atoms of the acetone molecule in **1a** were not included in the refinement.

QMB vapour sorption measurements

The experimental setup of the quartz crystal microbalance consists of two 10 MHz standard electronic quartzes with gold electrodes (FOQ Piezo Technik, Germany). One of them is uncoated and used as reference; the other one is coated with the receptor. Both quartzes are located in a thermostated metal block (controlled to 25 °C using a water thermostat). The measurements are carried out with a constant flow of synthetic air. The resonance frequencies of the quartzes are measured using a multi-channel frequency counter (HKR Sensor Systems, Munich, Germany) at a resolution of 1 Hz. The frequency data can be read by the computer *via* a serial interface, and the coating of the quartzes was performed by dipping the quartz into a 10 mM solution of compound **1** in chloroform–toluene (1 : 1). According to the Sauerbrey equation,[26] the measured frequency change is proportional to the increase in mass caused by the adsorbed solvent, which is given as percentage of the coating. Therefore the adsorption relates to the thickness of the coating, and the data meet the requirement for a reasonable comparison.

X-ray powder diffraction

X-ray powder diffraction measurements were performed using a Siemens D5000 powder diffractometer at room temperature using the CuK_α line.

Acknowledgements

We thank the German Ministry of Economics and Technology for generous research funding. T. G. thanks Monika Mazik for her inspirational mentoring.

Notes and references

1 P. A. Wright, *Microporous Framework Solids (RSC Materials Monographs)*, Royal Society of Chemistry, Cambridge, 2008.
2 J. W. Steed and J. L. Atwood, *Supramolecular Chemistry*, John Wiley & Sons, Chichester, 2nd edn, 2009.

3 K. E. Maly, *J. Mater. Chem.*, 2009, **19**, 1781.
4 R. W. Boyd, *Nonlinear Optics*, Academic Press, Oxford, 3rd edn, 2008.
5 *Handbook of Zeolite Science and Technology*, ed. S. M. Auerbach, K. A. Carrado and P. K. Dutta, CRC Press, 2003.
6 *Metal–Organic Frameworks: Design and Application*, ed. L. R. MacGillivray, Wiley, Hoboken, 2010.
7 *Metal–Organic Frameworks: Applications from Catalysis to Gas Storage*, ed. D. Farrusseng, Wiley-VCH, Weihnheim, 2011.
8 T. Hertzsch, J. Hulliger, E. Weber and P. Sozzani, Organic Zeolites, in *Encyclopedia of Supramolecular Chemistry*, ed. J. Atwood, J. Steed, Marcel Dekker, New York, 2004.
9 G. Couderc and J. Hulliger, *Chem. Soc. Rev.*, 2010, **39**, 1545.
10 H. Mansikkamäki, M. Nissinen and K. Rissanen, *Angew. Chem., Int. Ed.*, 2004, **43**, 1243; C. Tedesco, I. Immediata, L. Gregoli, L. Vitagliano, A. Immirzia and P. Neri, *CrystEngComm*, 2005, **7**, 449; F. Perret, A. D. Lazar, O. Shkurenko, K. Suwinska, N. Dupont, A. Navaza and A. W. Coleman, *CrystEngComm*, 2006, **8**, 890; S. Kennedy and S. J. Dalgarno, *Chem. Commun.*, 2009, 5275; S. J. Dalgarno, J. E. Warren, J. Antesberger, T. E. Glass and J. L. Atwood, *New J. Chem.*, 2007, **31**, 1891; C. Tedesco, L. Erra, M. Brunelli, V. Cipolletti, C. Gaeta, A. N. Fitch, J. L. Atwood and P. Neri, *Chem.–Eur. J.*, 2010, **16**, 2371; S. Kennedy, G. Karotsis, C. M. Beavers, S. J. Teat, E. K. Brechin and S. J. Dalgarno, *Angew. Chem., Int. Ed.*, 2010, **49**, 4205; C. Tedesco, L. Erra, I. Immediata, C. Gaeta, M. Brunelli, M. Merlini, C. Meneghini, P. Pattison and P. Neri, *Cryst. Growth Des.*, 2010, **10**, 1527; R. de Zorzi, N. Guidolin, L. Randaccio and S. Geremia, *CrystEngComm*, 2010, **12**, 4056; L. Erra, C. Tedesco, I. Immediata, L. Gregoli, C. Gaeta, M. Merlini, C. Meneghini, M. Brunelli, A. N. Fitch and P. Neri, *Langmuir*, 2012, **28**, 8511; G. Brancatelli, R. de Zorzi, N. Hickey, P. Siega, G. Zingone and S. Geremia, *Cryst. Growth Des.*, 2012, **12**, 5111; A. Arduini, R. Bussolati, C. Massera, A. Pochini, F. Rapaccioli, A. Secchi and F. Ugozzoli, *Supramol. Chem.*, 2013, **25**, 703–708.
11 B. Tomapatanaget, T. Tuntulani and O. Chailapakul, *Org. Lett.*, 2003, **5**, 1539; B. Tomapatanaget and T. Tuntulani, *Tetrahedron Lett.*, 2001, **42**, 8105; P. Timmerman, J.-L. Weidmann, K. A. Jolliffe, L. J. Prins, D. N. Reinhoudt, S. Shinkai, L. Frish and Y. Cohen, *J. Chem. Soc., Perkin Trans. 2*, 2000, 2077.
12 G. R. Desiraju and T. Steiner, *The Weak Hydrogen Bond in Chemistry and Structural Biology*, IUCr Monographs on Crystallography, Oxford University Press, Oxford, UK, 1999, vol. 9, p. 29.
13 S. G. Bott, A. W. Coleman and J. L. Atwood, *J. Am. Chem. Soc.*, 1986, **108**, 1709.
14 For typical examples, see: A. Soi, W. Bauer, H. Mauser, C. Moll, F. Hampel and A. Hirsch, *J. Chem. Soc., Perkin Trans. 2*, 1998, 1471; S. Kumar, R. Varadarajan, H. M. Chawla, G. Hundal and M. S. Hundal, *Tetrahedron*, 2004, **60**, 1001; T. Gruber, M. Gruner, C. Fischer, W. Seichter, E. Weber and P. Bombicz, *New J. Chem.*, 2010, **34**, 250, and references cited therein; C. Fischer, G. Lin, W. Seichter and E. Weber, *Tetrahedron*, 2011, **67**, 5656; C. Fischer, W. Seichter and E. Weber, *Beilstein J. Org. Chem.*, 2011, **7**, 1602; C. Fischer, P. Bombicz, W. Seichter, F. Katzsch and E. Weber, *Cryst. Growth Des.*, 2012, **12**, 2445; S. Kennedy, C. M. Beavers, S. J. Teat and S. J. Dalgarno, *Cryst. Growth Des.*, 2012, **12**, 679; C. Fischer, P. Bombicz, W. Seichter and E. Weber, *Struct. Chem.*, 2013, **24**, 535.
15 R. K. Juneja, K. D. Robinson, C. P. Johnson and J. L. Atwood, *J. Am. Chem. Soc.*, 1993, **115**, 3818; B. Klenke, C. Näther and W. Friedrichsen, *Tetrahedron Lett.*, 1998, **39**, 8967; I. Columbus and S. E. Biali, *J. Org. Chem.*, 2008, **73**, 2598; M. P. Hertel, A. C. Behrle, S. A. Williams, J. A. R. Schmidt and J. L. Fantini, *Tetrahedron*, 2009, **65**, 8657; C. Fischer, T. Gruber, W. Seichter and E. Weber, *Org. Biomol. Chem.*, 2011, **9**, 4347.
16 O. R. Pedireddi, D. S. Reddy, B. S. Goud, D. C. Craig, A. D. Rae and G. R. Desiraju, *J. Chem. Soc., Perkin Trans. 2*, 1994, 2353; F. F. Awwadi, R. D. Willett, K. A. Peterson and B. Twamley, *Chem.–Eur. J.*, 2006, **12**, 8952.
17 P. K. Thallapally and A. Naugia, *CrystEngComm*, 2001, **3**, 114; L. Brammer, E. A. Bruton and P. Sherwood, *Cryst. Growth Des.*, 2001, **1**, 277.
18 C. Fischer, T. Gruber, D. Schindler, W. Seichter and E. Weber, *Cryst. Growth Des.*, 2011, **11**, 1989.
19 T. Harada, J. M. Rudziński and S. Shinkai, *J. Chem. Soc., Perkin Trans. 2*, 1992, 2109.
20 W. Verboom, A. Durie, R. J. M. Egberink, Z. Asfari and D. N. Reinhoudt, *J. Org. Chem.*, 1992, **57**, 1313.
21 A. Janshoff, H.-J. Galla and C. Steinem, *Angew. Chem., Int. Ed.*, 2000, **39**, 4004; K. Matsuura, K. Ariga, K. Endo, Y. Aoyama and Y. Okahata, *Chem.–Eur. J.*, 2000, **6**, 1750; U. Schramm, C. E. O. Roesky, S. Winter, T. Rechenbach, P. Boeker, P. Schulze Lammers, E. Weber and J. Bargon, *Sens. Actuators, B*, 1999, **57**, 233.
22 L. S. Yakimova, M. A. Ziganshin, V. A. Sidorov, V. V. Kovalev, E. A. Shokova, V. A. Tafeenko and V. V. Gorbatchuk, *J. Phys. Chem. B*, 2008, **112**, 15569.
23 J. van Loon, A. Arduini, L. Coppi, W. Verboom, A. Pocchini, R. Ungaro, S. Harkema and D. N. Reinhoudt, *J. Org. Chem.*, 1990, **55**, 5639.
24 *SADABS, Siemens Area Detector Absorption Correction Program*, Bruker AXS Inc., Madison, Wisconsin, USA, 2007.
25 G. M. Sheldrick, *Acta Crystallogr., Sect. A: Found. Crystallogr.*, 2008, **64**, 112.
26 G. Sauerbrey, *Z. Phys.*, 1959, **155**, 206.

